ECCOMAS Congress 2016
VII European Congress on Computational Methods in Applied Sciences and Engineering
M. Papadrakakis, V. Papadopoulos, G. Stefanou, V. Plevris (eds.)
Crete Island, Greece, 5–10 June 2016

NUMERICAL INVESTIGATION OF THERMOACOUSTIC ENGINE USING IMPLICIT LARGE EDDY SIMULATION

M. Mahdaoui[1,2], R. Bennacer[2] and S. Kouidri[1, 3], N. Martaj [4]

[1] LIMSI-CNRS
BP 133, 91403 Orsay Cedex, France
Mahdaoui@limsi.fr

[2] LMT /ENS-Cachan/CNRS/Université Paris Saclay,
61 avenue du Président Wilson, 94235 Cachan, France
Rachid.bennacer@ens-cachan.fr

[3] Sorbonne University, UPMC Univ, Paris 6
UFR 919, 75005 Paris, France
Smaine.Kouidri@limsi.fr

[4] EPF Campus de Troyes
2, rue F. Sastre 10430 Rosières-près-Troyes, France
nadia.martaj@epf.fr

Keywords: Thermoacoustic engine, Acoustic streaming, Implicit Large Eddy Simulation, CFD.

Abstract. *Thermoacoustic engines are device that converts heat energy into work in the form of acoustic energy. The energy conversion using thermoacoustic techniques has the advantages of constructional simplicity, absence of moving parts, reliable operation, long service life and no environmental pollution. However, efficiency of thermoacoustic systems still needs to be improved (which is typically 40% of the Carnot coefficient of performance).*
To improve the efficiency of thermoacoustic engine, a thorough understanding of the flows in machines, onset temperature, acoustic velocity and streaming velocity is necessary. In this study, numerical simulation of a thermoacoustic heat engine is performed. The possibility of using Implicit Large Eddy Simulation (ILES) to simulate the flows in the thermoacoustic engine has been examined by using COMSOL Multiphysics. Unlike the Large Eddy Simulation (LES), ILES is neither explicit filtering nor explicit subgrid model: small-scale fluctuations are damped by the numerical diffusion, which acts both as an implicit filter and an implicit built-in subgrid model for a given grid. As the grid is refined, the simulation converges to a DNS.
The results show that the ILES has predicted flows in the thermoacoustic engine and especially time-averaged flow called acoustic streaming, which can lead to undesired heat convection and loss of efficiency.

1 INTRODUCTION

The thermoacoustic machines are a new type machines based on the interaction between the thermodynamic and acoustic phenomena. In recent years, these machines occupy an important place in both the industrial development and in the comfort of habitat. This diversification of the mode of use of thermoacoustic machines is due to a number of benefits, recorded on these machines: no moving parts, high reliability and low environmental friendliness compared with traditional heat engine. [1-3]. However, efficiency of thermoacoustic systems still needs to be improved, especially for the standing wave thermoacoustic engine (which is typically 40% of the Carnot coefficient of performance (Swift [3])) and their performance needs to be better understood. To improve the efficiency of thermoacoustic engine and refrigerators apart from improved resonator, stack and loudspeaker design, it is necessary to better understand the flow and thermal fields. Many strategies are proposed to improve the efficiency of thermoacoustic machines.

In thermoacoustic devices, the energy is carried by an acoustic wave. This acoustic wave can induce a time-averaged flow, called acoustic streaming, which can lead to undesired heat convection and loss of efficiency. Different classes of acoustic streaming can be distinguished based on the underlying physical mechanisms. Rayleigh streaming, as first analytically described by Lord Rayleigh in 1884 [4], is the phenomenon of a net mean flow in a standing wave resonator driven by the viscous stresses close to the solid boundary [5]. In the traveling-wave thermoacoustic engine usually has a loop configuration, which may cause an acoustic streaming named as Gedeon streaming [6].

Acoustic streaming can have a large impact on the performance of thermoacoustic prime movers and refrigerators as the generated mean flow can lead to undesirable mean convective heat transport [7, 8]. There are many experimental and theoretical studies to better understand and to suppress acoustic streaming [8-14]. They investigated mechanisms of streaming generation, and they introduced elements to suppress the streaming like a jet pump and phase adjuster.

Several numerical calculations recently addressed the modeling of the flow field inside a thermoacoustic couple [15-19]. Cao et al. [15] presented numerical simulations of the flow behavior in the thermoacoustic couple, and calculated the energy flux density in a parallel-plate stack.

To understand the evolution of the physical parameters (pressure, velocity, streaming, etc.) in thermoacoustic engine, a 2D model was used in view of the geometric configuration of the machine. This model is based on solving the Navier Stokes equations, the heat equation and the ideal gas equation. The Implicit Large Eddy Simulation (ILES) was used to simulate the flows in thermoacoustic machine [20-22]. This method uses the full Navier-Stokes equations instead of Reynolds Averaged Navier-Stokes (RANS) and does not use an explicit turbulence model. Unlike the Large Eddy Simulation (LES), ILES is neither explicit filtering nor explicit subgrid model: small-scale fluctuations are damped by the numerical diffusion, which acts both as an implicit filter and an implicit built-in subgrid model for a given grid. As the grid is refined, the simulation converges to a DNS. ILES is an effective method for transitional flows, especially when coupled with heat transfer. It captures accurately the energy exchanges between various modes, namely convective, acoustic and thermal, in a wide range of velocity and turbulence intensity.

2 PHYSICAL AND NUMERICAL MODEL

The thermoacoustic engine illustrated in Fig. 1 is made of a resonator, opened to the environment on its one side, a stack and two heat exchangers whose function is to create an appropriate thermal gradient. A standing acoustic wave is generated in the device. Its velocity node is at the closed end of the tube and the velocity antinode – at the opened cross section of the engine. The stack, of length 10mm, formed by a stack of rectangular plates of 0.5 mm wide and spaced 0.5mm between them. Our model problem is similar to the one considered in [17].

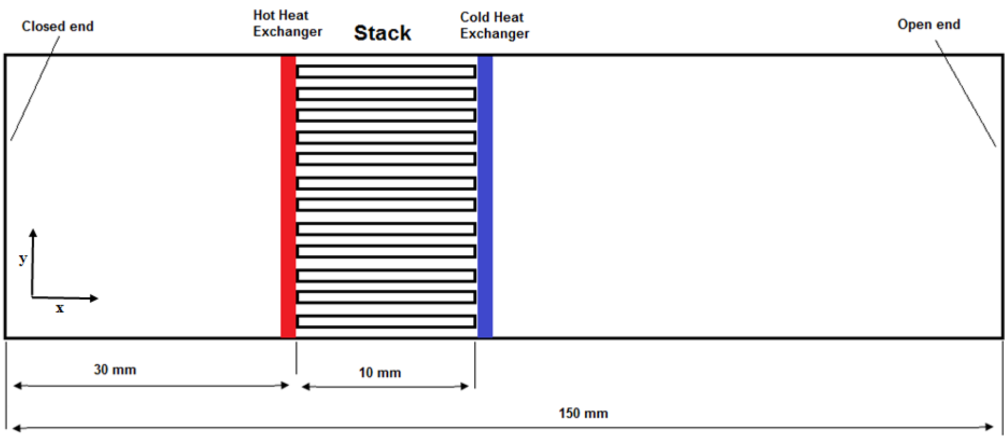

Figure 1: The thermoacoustic engine and its basic components.

To model the thermoacoustic generator, we used the mass conservation, momentum, energy equations and the equation of state.
The evolution of pressure, velocity and density is governed by the Navier-Stokes equations applied to the gas circulating in the resonator and in the stack.

$$\frac{\partial \rho}{\partial t} + \nabla \cdot (\rho u) = 0 \tag{1}$$

$$\rho \left(\frac{\partial u}{\partial t} + (u \cdot \nabla)\, u \right) = \nabla \cdot [-p \ I + \mu\, (\nabla u + (\nabla\, u)^T) - \frac{2}{3}\, \mu\, (\nabla \cdot u) I] + F \tag{2}$$

The energy equation used is as follows:

$$\rho C_P \left(\frac{\partial T}{\partial t} + u \cdot \nabla T \right) = \nabla \cdot (k \nabla T) + Q_{vh} + W_p \tag{3}$$

Where W_p is the pressure work term and Q_{vh} is the contribution of viscous heating given by:

$$W_p = \alpha_p T \left(\frac{\partial p_A}{\partial t} \right) \tag{4}$$

$$\alpha_p = -\frac{1}{\rho} \left(\frac{\partial \rho}{\partial T} \right)\Bigg|_p \tag{5}$$

$$Q_{vh} = \tau : \nabla u \tag{6}$$

α_p is thermal expansion coefficient.
To solve the system of partial differential equations described above, it is necessary to provide additional equation, linking the physical parameters of the fluid.
We consider the following state of the ideal gas equation for the working gas (air):

$$\rho = \frac{P_A}{R_S T} \tag{7}$$

Firstly, a steady simulation was performed with 10 Pa pressure as inlet condition at the closed end of the resonator and atmospheric pressure at the output of the resonator.

In the present study, all walls are adiabatic, except horizontal surfaces in the stack. The boundary condition of the temperature along such horizontal stack surfaces is determined by the following expression:

$$T(x) = 500 - 200 \ \cos(\pi \frac{x_{stack}}{L_{st}}) \tag{8}$$

This steady simulation was used to introduce pressure disturbance and an initial flow for transient simulation. In this case, adiabatic wall replaced pressure inlet condition on the compliance side.

A mesh based triangular elements was used with a total cell number of about 160000 cells. The mesh was refined near wall in the boundary viscous layer of the stack. The resolution of this boundary layer is necessary since the formation of acoustic streaming is principally induced by the interaction between the acoustic wave and the viscous boundary.

3 RESULTS ANS DISCUSSION

The model described above is used to study a thermoacoustic engine using the implicit large eddy simulation implemented in COMSOL Multiphysics software. As implicit modeling we denote the situation when the unmodified conservation law is discretized and the numerical truncation error acts as an SGS model. Since this SGS model is implicitly contained within the discretization scheme, an explicit computation of model terms becomes unnecessary.

The process of the acoustic wave excitation is presented in Fig 2. The basic time step of 10^{-5} second was adopted for the unsteady calculations. It can be noticed that in the initial stage of the pressure oscillation stems from an initial disturbance until the balance between the acoustic power dissipation and acoustic power generation is reached. The peak-to-peak value of thermoacoustic oscillation was 8 kPa. The FFT analysis of the pressure oscillation is shown in the Fig. 3. The main frequency component is equal to about 614 Hz and is in a good agreement with results of [17]. Two additional harmonics, at 1222 Hz and 1830 Hz are visible.

Fig. 4 shows the acoustic velocity distribution, u, versus time at fixed position of x= 20 mm, the velocity amplitude at this position is about 2.5 m/s. The acoustic velocity u along the length of the thermoacoustic engine for individual phase of half period T/2 of oscillation is presented in Fig. 5. The characteristics were determined along the line y= 4.23mm. We find that the acoustic velocity is maximum at x = 30mm and equal to 11m / s. This maximum value is due to the presence of the stack, which generates a constricting section. The velocity amplitude was determined at the open end of the device where the velocity antinode located.

To study the distribution of pressure in the thermoacoustic engine Figs. 6 and 7 present the acoustic pressure p distribution in function of time at x= 20 mm and The acoustic pressure u along the length of the thermoacoustic engine for individual phase of half period Tp/2 of oscillation along the line y =4.23mm. In the close end of the device, the pressure amplitude is equal 4 kPa in this place the pressure antinode appears. It can also be noticed in the outlet section of the thermoacoustic engine a pressure node is located.

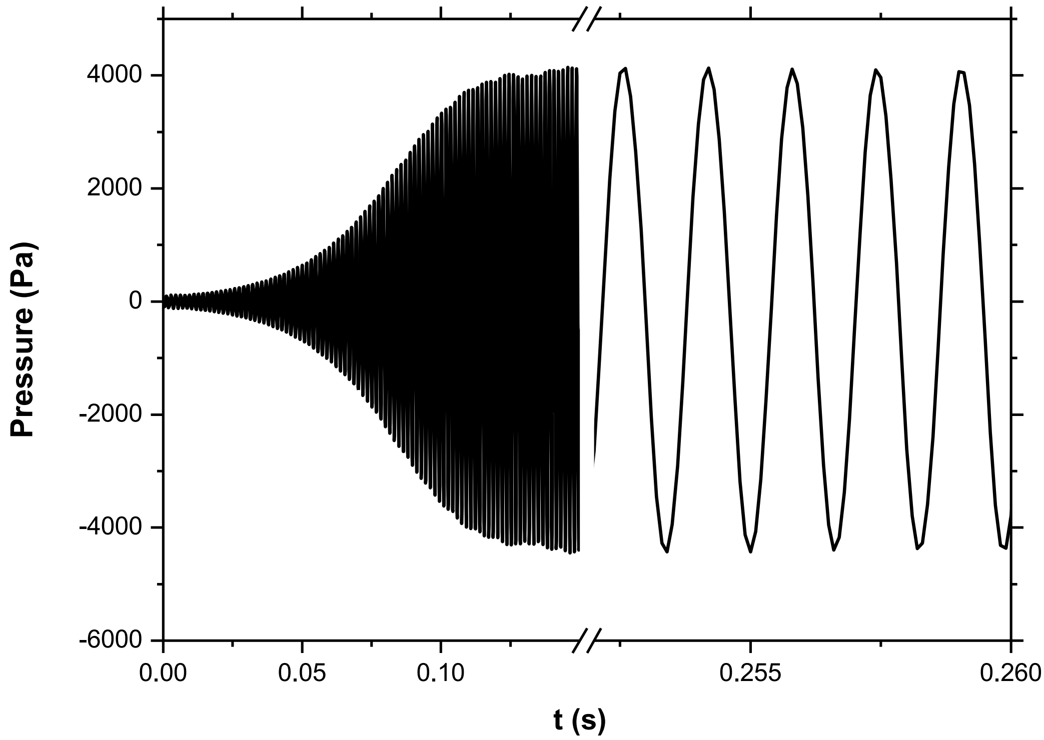

Figure 2: The evolution of the pressure oscillation at a x= 20mm.

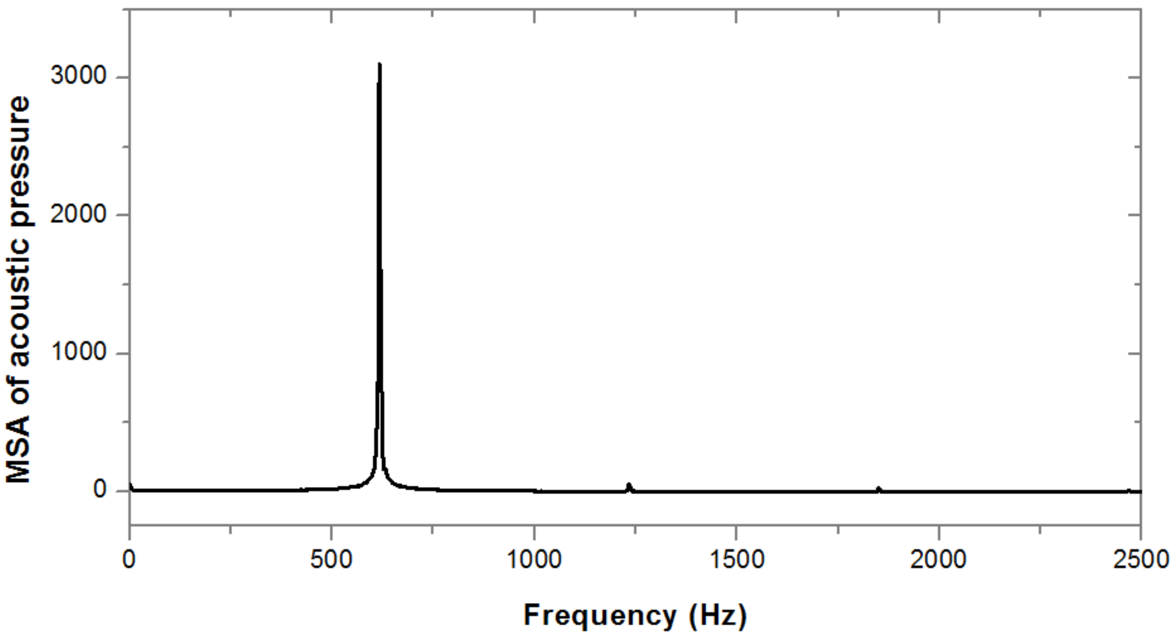

Figure 3: FFT analysis of the pressure oscillation.

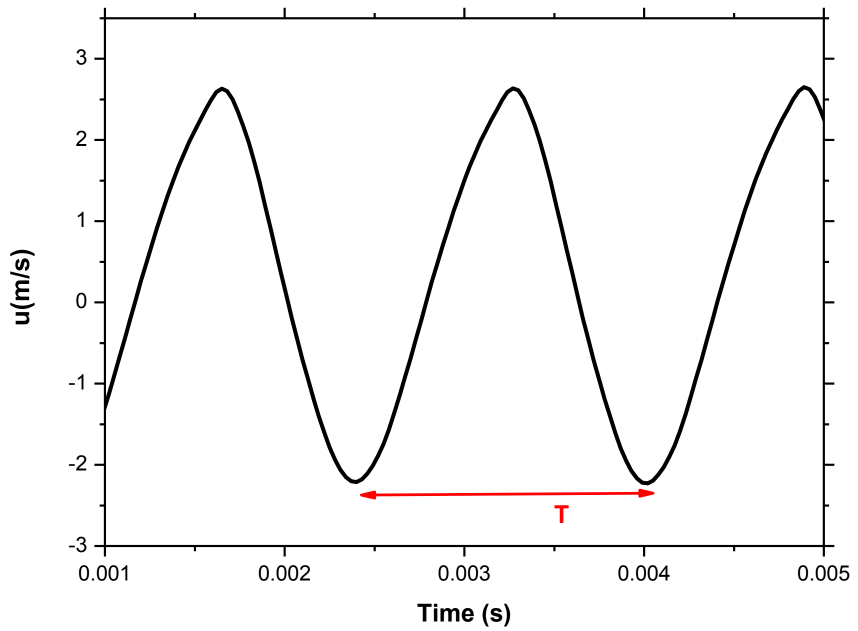

Figure 4: Time evolution of the acoustic velocity at a point in the vicinity of the stack.

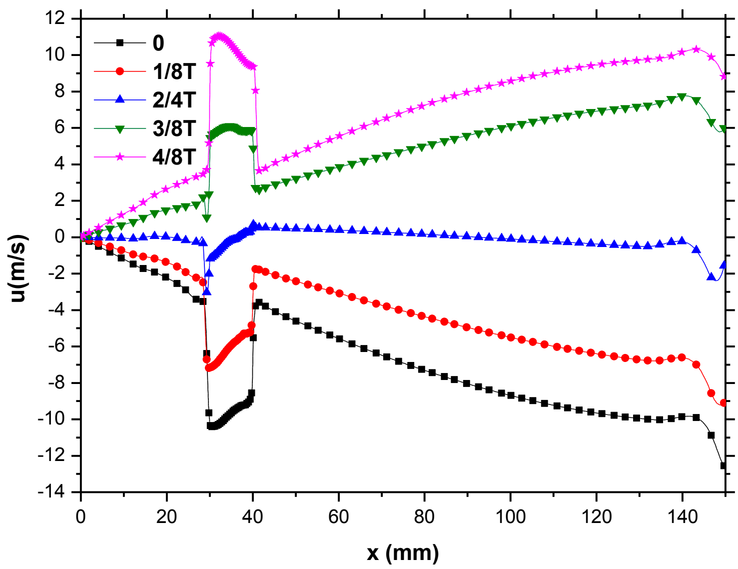

Figure 5: Distribution of instantaneous velocity depending on the length of thermoacoutic engine.

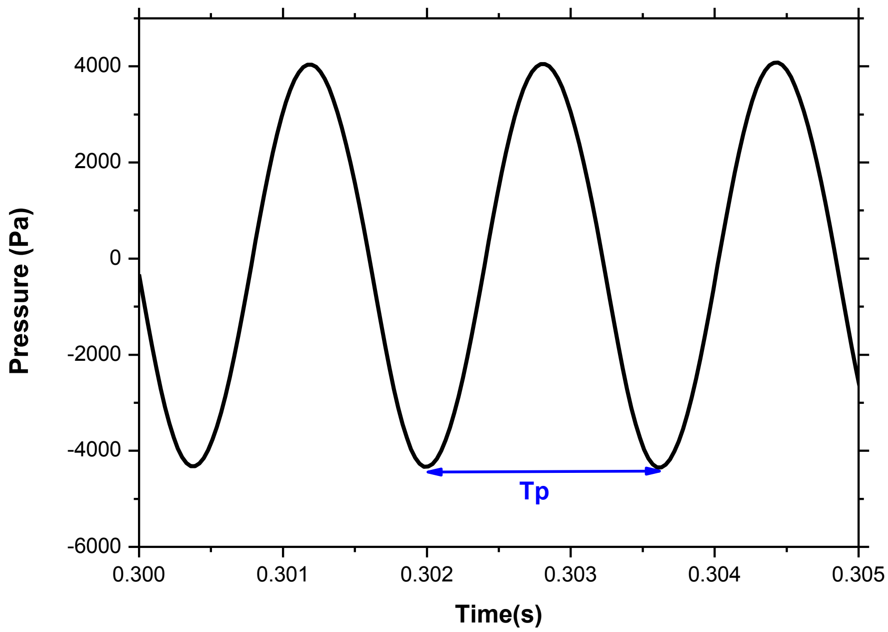

Figure 6: The evolution of the pressure oscillation.

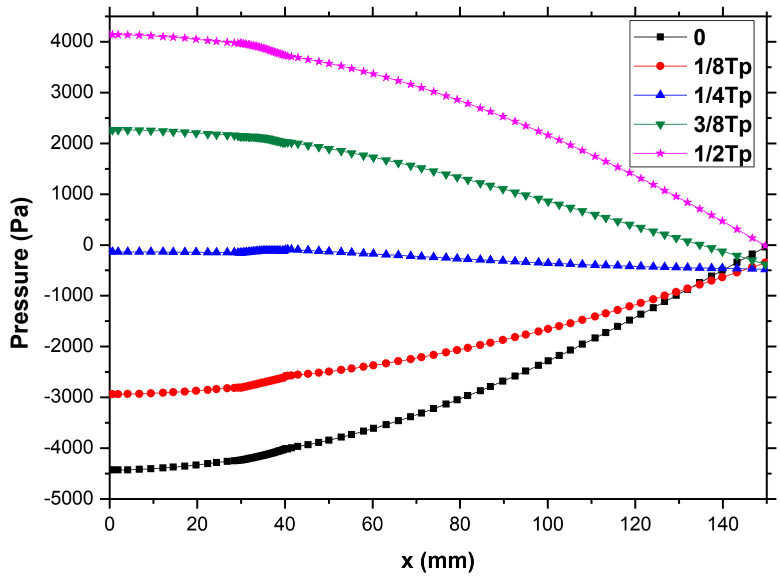

Figure 7: Distribution of instantaneous pressure depending on the length of thermoacoutic engine.

Secondary flows are mean flows that reduces the energy efficiency of thermoacoustic machine by creating thermal bridges particularly between stack ends. Fig. 8 depicts the cycle averaged flow field in the thermoacoustic engine. These steady flow structures (acoustic streaming) are computed from on the average mass transport velocities defined as;

$$u_2 = \frac{\langle \rho u \rangle}{\langle \rho \rangle} \qquad v_2 = \frac{\langle \rho v \rangle}{\langle \rho \rangle} \tag{10}$$

Here u_2 and v_2 are components of the acoustic streaming velocity. The instantaneous density, u and v values are time averaged during the 60th cycle and the streaming velocities obtained at the time which the mass transport velocities reach quasi steady values and do not change with increasing number of periods.

From Fig. 8 it can be seen that there are several secondary flow into the machine. These streaming appear in the resonator of thermoacoustic engine and near close end. Also small vortex are seen next to the stack and between the plates of the stack. These streaming reduce the useful gradient and therefore the engine efficiency. To make a quantitative study of streaming velocity, the profile of u_2 was plotted for three different axial positions as illustrated in Fig. 9. From this figure, it can be seen the symmetry of the streaming velocity curves over the axis that passes through the engine center. the acoustic velocity varies between 0.3 m/s and -0.3 m/s. In both areas, next to the stack, we plotted the velocity profile along y (see Fig. 10). After this analysis, the ability of the ILES approach to capture the small structures in the oscillating flow in the thermoacoustic engine is confirmed.

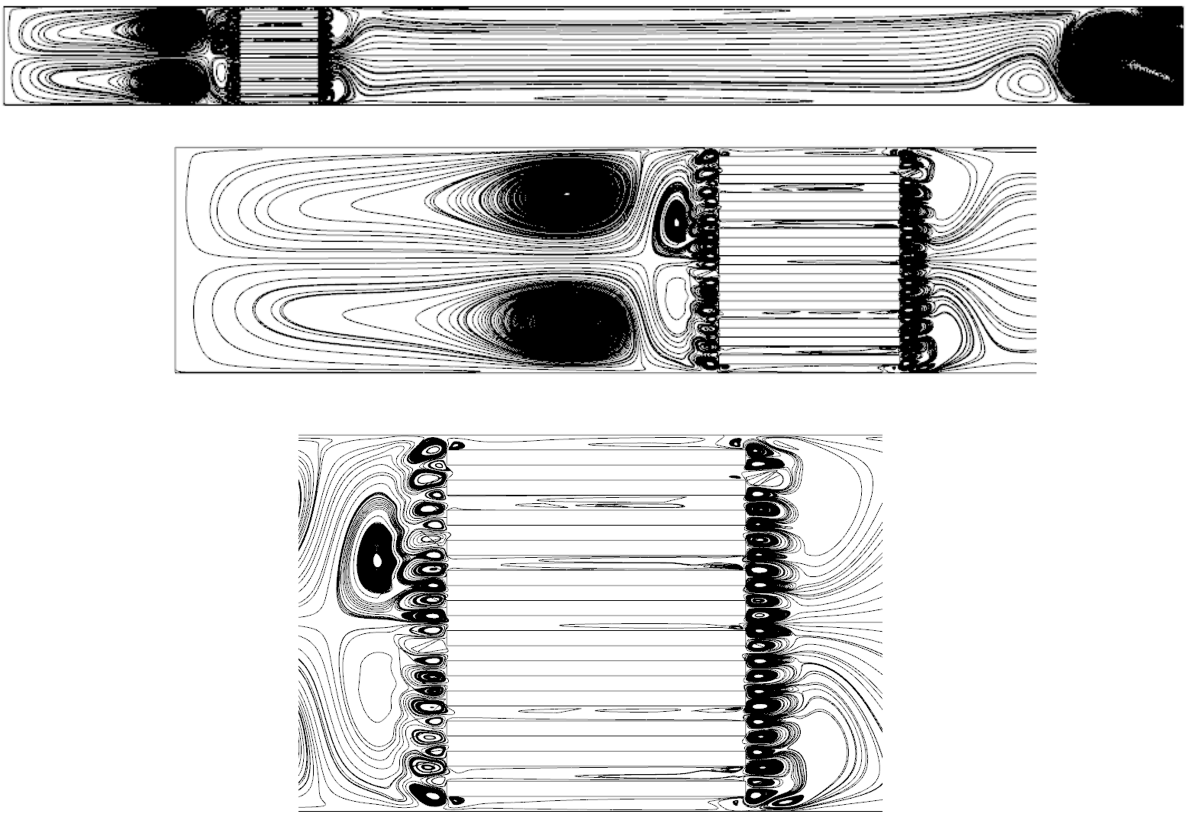

Figure 8: Stream line for streaming velocity

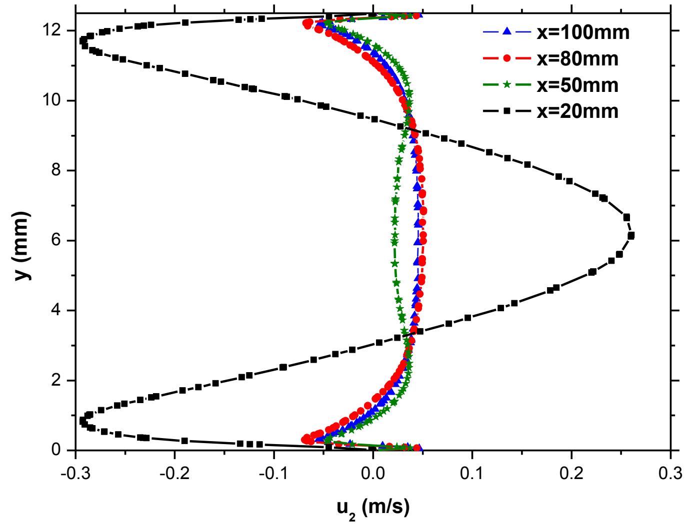

Figure 9: Streaming velocity profile u_2 at three axial positions.

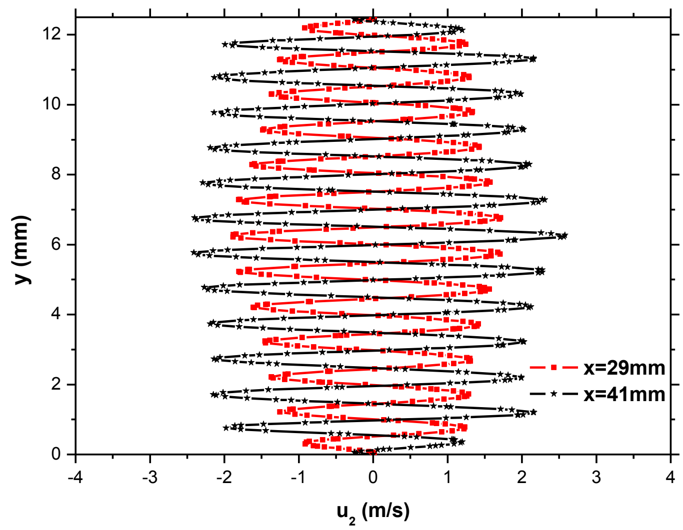

Figure 10: Streaming velocity profil at two positions near the stack**.**

4 CONCLUSIONS

This work presents the study of streaming velocity in a thermoacoustic engine using Implicit Large Eddy Simulation. The model used is based on solving the Navier Stokes equations, the heat equation and the ideal gas equation. First order velocity and second order velocity (streaming velocity) are obtained and analyzed. The results show that the ILES has predicted flows in the thermoacoustic engine and particularly acoustic streaming, which can lead to undesired heat convection and loss of efficiency. These streaming appear into thermoacoustic engine, especially between the plates of the stack.

REFERENCES

[1] G.W. Swift, Thermoacoustic engines, *Journal of the Acoustical Society of America 84* 1145–1180, 1988.

[2] J.C. Wheatly, T. Hofler, G.W. Swift, A. Miglori, Understanding some simple phenomena in thermoacoustics with applications to acoustical heat engines, *American Journal of Physics 53,* 147–162, 1985.

[3] G.W. Swift, Thermoacoustic engines and refrigerators, *Physics Today*, 22–28, 1995.

[4] L Rayleigh, On the circulation of air observed in Kundt's tubes, and on some allied acoustical problems, *Philosophical Transactions of the Royal Society of London* 175, 1–21, 1884.

[5] S. Boluriaan and P. J. Morris, Acoustic streaming: from Rayleigh to today, *International Journal of Aeroacoustics* 2, 255–292, 2003.

[6] D. Gedeon, *DC gas flows in Stirling and pulse tube cryocoolers*. In: Ross Jr RG, editor. Cryocoolers 9. New York: Plenum Press, p. 385–92, 1997.

[7] S. Backhaus, GW. Swift, A thermoacoustic Stirling heat engine. *Nature*, 399(6734), 335–8, 1999.

[8] S. Backhaus, GW. Swift. A thermoacoustic-Stirling heat engine: detailed study. *J Acoust Soc Am*, 107(6), 3148–66, 2000.

[9] N. Rott, Thermoacoustics, *Adv. Appl. Mech*. 20, 135–175, 1980.

[10] MF. Hamilton, YA Ilinskii, EA Zabolotskaya. Thermal effects on acoustic streaming in standing waves. *J Acoust Soc Am*,114:3092–101, 2003.

[11] IE. Idelchik *Handbook of hydraulic resistance*. *3rd ed*. New York: Begell House; 1996.

[12] R. Paridaens, S. Kouidri, & F. J. Jerbi, Investigation on the generation mechanisms of acoustic streaming in a thermoacoustic prime mover. *Cryogenics*, 58, 78-84, 2013.

[13] Y. W. Liu, & P. Yang, Influence of inner diameter and position of phase adjuster on the performance of the thermo-acoustic Stirling engine. *Applied Thermal Engineering*, 73(1), 1141-1150, 2014.

[14] M. Chen, & Y. L. Ju, Effect of different working gases on the performance of a small thermoacoustic Stirling engine. *International Journal of Refrigeration*, 51, 41-51, 2015.

[15] N. Cao, JR. Olson, GW. Swift, S. Chen, Energy flux density in a thermoacoustic couple. *J Acoust Soc Am*, 99(6):3456–64, 1996.

[16] N. Lycklama, J. L., M. E. H. Tijani, & S. Spoelstra. Simulation of a traveling-wave thermoacoustic engine using computational fluid dynamics. *The Journal of the Acoustical Society of America*, 118(4), 2265-2270, 2005.

[17] F. Zink, J. Vipperman, & L. Schaefer, CFD simulation of a thermoacoustic engine with coiled resonator. *International Communications in Heat and Mass Transfer*, 37(3), 226-229, 2010.

[18] S. H. Tasnim & R. A. Fraser, Computation of the flow and thermal fields in a thermoacoustic refrigerator. *International Communications in Heat and Mass Transfer*, *37*(7), 748-755, 2010.

[19] G. Yu, W. Dai, & E. Luo, CFD simulation of a 300Hz thermoacoustic standing wave engine. *Cryogenics*, *50*(9), 615-622, 2010.

[20] F.F. Grinstein, L.G. Margolin, W.J. Rider, *Implicit Large Eddy Simulation*, Cambridge University Press, 2007.

[21] COMSOL Multiphysics 5.1, *COMSOL Reference Guide*, 2015.

[22] M. Hashiguchi, Possibility of Implicit LES for Two-Dimensional Incompressible Lid-Driven Cavity Flow Based on COMSOL Multiphysics. *Accessed online* 11, 2015.